JCTC Journal of Chemical Theory and Computation

Letter

pubs.acs.org/JCTC

Excited-State Geometries of Solvated Molecules: Going Beyond the Linear-Response Polarizable Continuum Model

Siwar Chibani,[†] Adèle D. Laurent,[†] Aymeric Blondel,[†] Benedetta Mennucci,*[,‡] and Denis Jacquemin*[,†,§]

[†]Laboratoire CEISAM - UMR CNRS 6230, Université de Nantes, 2 Rue de la Houssinière, BP 92208, 44322 Nantes Cedex 3, France

[‡]Department of Chemistry, University of Pisa, Via Risorgimento 35, 56126 Pisa, Italy

[§]Institut Universitaire de France, 103, bd Saint-Michel, F-75005 Paris Cedex 05, France

Supporting Information

ABSTRACT: The theoretical determination of excited-state structures remains an active field of research, as these data are hardly accessible by experimental approaches. In this contribution, we investigate excited-state geometries obtained with Time-Dependent Density Functional Theory, using both linear-response and, for the first time, corrected linear-response approaches of the Polarizable Continuum Model. Several chromophores representative of key dye families are used. In most cases, the corrected linear-response approach provides bond distances in between the gas and linear-response data, the latter model providing larger medium-induced structural changes than the corrected linear-response model. However, in a few cases, the solvation effects predicted by the two continuum approaches present opposite directions compared to the gas phase reference.

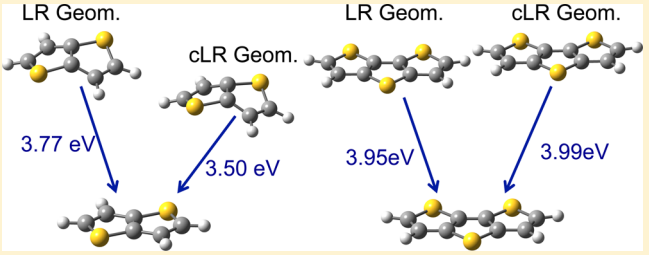

Time-Dependent Density Functional Theory (TD-DFT),[1] and more precisely, its adiabatic approximation,[2] has become the *de facto* standard method for exploring excited states of medium and large molecules.[3] Besides its computational efficiency, this popularity can be explained, on the one hand, by the availability of first and second TD-DFT derivatives making the efficient exploration of the excited-state potential energy surface possible[4−6] and, on the other hand, by the development of a panel of variants of the Polarizable Continuum Model (PCM) allowing to rapidly model solvent effects.[7−11] In particular, the linear response (LR),[7,8] corrected linear response (cLR),[9] and state specific (SS)[10] PCM approaches have been implemented in widely available TD-DFT package(s), whereas the vertical excitation model (VEM) is a recently proposed alternative.[11] All these models represent the solvent polarization in terms of induced charges on the surface of a cavity embedding the dye; however, the way this polarization changes from the ground to the excited state differs. In the LR scheme, the transition densities are used to determine the change in the PCM charges. In the cLR scheme, the one-particle TD-DFT density matrix, that accounts for the orbital relaxation contribution, is used in a perturbation approach. In the SS scheme, a self-consistent formulation is used, but at the price of a modification of the ground-state reference. VEM is also self-consistent and state-specific, but it does not involve modifying the ground state.[11] For most cases, and more specifically for fluorescence, both cLR and SS provide a more physically sound description of the excited-state phenomena than their LR counterpart. Since 2006, one can even combine the calculation of TD-DFT gradients with PCM,[12] but only within the LR approach. Therefore, a common procedure to determine fluorescence of solvated dyes is to use LR-PCM to determine the excited-state structures and, next, to perform single point vertical cLR/SS-PCM calculations on these geometries. While this procedure is apparently valid, it may only hold if the effects that are not included in the LR approach are captured by the vertical transition energy and only marginally affect the geometry of the emissive state. This is probably reasonable when the LR description is qualitatively correct, but we have recently explored several series of organic dyes for which larger differences between the LR and cLR/SS vertical transition energies have been found.[13−15] This, in turn, indicates a possible significant modification of the excited-state potential energy surfaces. Therefore, in this communication, we aim to model excited states using the cLR approach not only to compute transition energies but also to optimize the geometrical parameters in a fully consistent approach. Our goal is therefore to appraise the validity of the LR-PCM approach for optimizing excited-state geometries. To the best of our knowledge, this is the first work going beyond LR-PCM for optimizing excited-state geometries with TD-DFT.

All calculations have been performed with the latest version of the Gaussian 09 program (modified for cLR optimization, see below).[16] We have systematically applied an improved energy convergence threshold (at least 10^{-10} a.u.), a tight geometry optimization criterion (10^{-5} a.u. on the residual root-

Received: February 20, 2014
Published: March 24, 2014

Table 1. Relevant Excited-State Parameters Obtained for Hydrogen Cyanide (Unconstrained) and Butadiene (Constrained to C_{2h})[19] Using Different Computational Approaches[a]

			hydrogen cyanide			butadiene		
functional	solvent	method	H−C	C≡N	H−C≡N	$C-C_{ext}$	$C-C_{int}$	C−C−C
B3LYP		gas	1.125	1.304	122.6	1.383	1.415	121.9
	toluene	LR	1.121	1.305	122.8	1.428	1.398	124.5
		cLR	1.123	1.304	122.9	1.383	1.414	121.8
	dichloromethane	LR	1.119	1.306	122.9	1.431	1.393	124.5
		cLR	1.121	1.304	123.2	1.383	1.414	121.8
	water	LR	1.118	1.307	122.9	1.432	1.391	124.5
		cLR	1.120	1.305	123.4	1.382	1.414	121.8
CAM-B3LYP		gas	1.118	1.299	122.7	1.420	1.392	124.3
	toluene	LR	1.115	1.300	122.8	1.423	1.387	124.3
		cLR	1.116	1.299	123.0	1.420	1.393	124.2
	dichloromethane	LR	1.113	1.301	122.9	1.427	1.382	124.3
		cLR	1.115	1.300	123.3	1.420	1.393	124.1
	water	LR	1.113	1.301	123.0	1.428	1.380	124.3
		cLR	1.114	1.300	123.4	1.421	1.392	124.1

[a]Bond lengths are in Å and valence angles in degrees. All values have been computed with 6-31++G(d,p).

mean-square force), and a high-level DFT integration grid (so-called *ultrafine* grid) in order to ensure the numerical stability of the presented data. Default parameters have been used for the PCM cavity, whereas several functionals, atomic basis sets, and solvents have been tested (see below). TD-DFT optimizations in the gas phase have been performed with the analytical gradients implemented in Gaussian 09, and the same holds for the LR-PCM excited-state calculations. For the latter, it was checked that the obtained structures correspond to true minima of the potential energy surface by numerically differentiating the LR-PCM-TD-DFT forces. cLR calculations require the access to the TD-DFT density, and as the geometrical derivatives of this density are not available in Gaussian09, the cLR optimizations have been performed through a numerical *eigenvalue-following* algorithm[17] starting from the optimal LR structures. However, to ensure a correct optimization, we had, on the one hand, to slightly modify the program to obtain the storage of the cLR energy in the adequate vector and, on the other hand, to use a nonstandard route as input. The validity of the computed numerical forces has been tested.[18] In this letter, the geometry optimizations have been performed in the equilibrium PCM limit, whereas the reported emission wavelengths are computed in the nonequilibrium PCM limit.

We have first tested the approach on two simple models: the first excited states of hydrogen cyanide and butadiene.[19] The results obtained with two exchange correlation functionals and the 6-31++G(d,p) atomic basis set can be found in Table 1, whereas 6-31G(d) results are given in the Supporting Information (SI). The H−C bond in hydrogen cyanide tends to contract in solvent, and this effect increases with solvent polarity for both functionals; CAM-B3LYP delivers more contracted bond lengths but with a similar evolution with solvation than the one obtained with B3LYP. Both LR and cLR give the same trend, but the cLR values are systematically closer to the gas phase data. The same holds for the slight elongation of the triple bond. For butadiene, an apolar molecule, one notices very small solvent effects and an almost perfect match between cLR and gas phase values, whereas LR data slightly differ with CAM-B3LYP and strongly differ with B3LYP. Indeed, with the selected basis set, LR-PCM calculations with B3LYP lead to a reversal of the bonding character of the two bonds (this is not true with 6-31G(d), see the SI). This is probably an artifact of the B3LYP exchange-correlation functional, a topic clearly beyond our scope here.

Let us now turn toward representative systems of actual organic dyes. The six treated molecules are displayed in Figure 1: **I** is the diketopyrrolopyrrole core, an increasingly popular

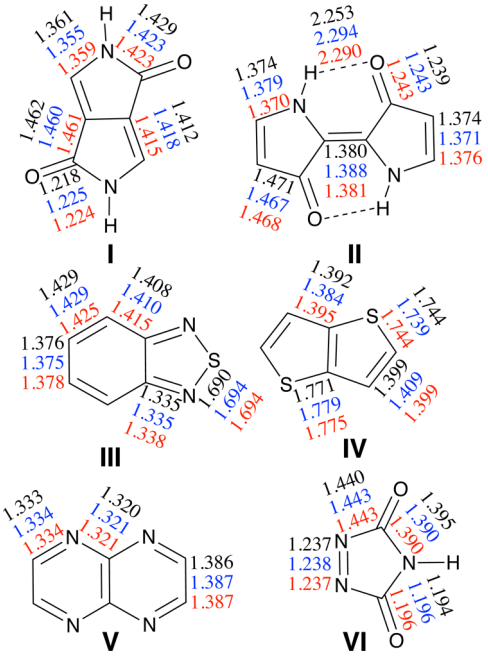

Figure 1. Sketch of the investigated model dyes. Selected bond lengths (Å) computed at the TD-M06-2X/6-31G(d) level are given for optimal gas (black) LR-PCM (blue) and cLR-PCM (red) structures. For PCM calculations, dichloromethane was systematically used as a solvent, and the equilibrium limit applied.

moiety in solar cell applications; **II** is the H-shaped chomophore of indigo, a classical organic dye; **III** is 2,1,3-benzothiadiazole, a strong acceptor undergoing a charge-transfer between the six- and five-membered cycles upon light absorption; **IV** is thieno[2,3-*b*]thiophene, a fragment present in several organic electronic devices; **V** and **VI** are two aza

dx.doi.org/10.1021/ct5001507 | J. Chem. Theory Comput. 2014, 10, 1848−1851

compounds used here as examples of $n \rightarrow \pi^*$ chromogens (the four other molecules presenting a $n \rightarrow \pi^*$ transition at lower energy). For the calculations on those compounds, we have used the M06-2X/6-31G(d) method and considered dichloromethane, a common solvent in dye chemistry. M06-2X has been shown to be an adequate exchange-correlation functional for investigating excited-state energies and structures.[20−27] Selected representative bond distances can be found in Figure 1.

For the selected rather rigid molecules, the variations induced by the environment on the excited-state bond lengths remain rather limited, ca. 0.005 Å though larger variations can be found for some specific bond lengths, e.g., the external C═C bond in **IV** and the intramolecular hydrogen bond in **II**. No systematic variations (elongation/contraction) of bond lengths can be detected when going from the gas to condensed phase. Let us focus on the evolution from the gas phase to solvent as described by the LR and cLR models. Overall, the variations of bond lengths induced by solvation are predicted to present the same sign with both LR and cLR for the majority of cases shown in Figure 1. It is also clear that the cLR distances typically lie in between the gas and LR bond lengths. We nevertheless note several exceptions to this general behavior, especially in **II** (both C−N and external C═C bonds) and in **IV**, in which cLR and LR predict opposite geometrical deformations compared to the gas phase reference. Moreover, **IV** is a nonplanar molecule in its excited state, and the central C−C−C−C dihedral angle is similar with the cLR and gas-phase models (129° and 131°, respectively), but is larger with the LR method (139°).

These trends are also reflected in the energy data collected in Table 2. In that table, we report the fluorescence energies, ω_{fluo}, obtained with cLR but using different geometries (gas-phase, LR and cLR) and the differences in the excited state cLR absolute energies, ΔE, due to the different selection of geometries (the reference value being the energy of the cLR optimized system). ΔE is a direct quantification of the purely geometrical effect. As it can be seen from the ΔE values, the effects of the different geometries are rather small, especially for the two $n \rightarrow \pi^*$ dyes, and attain a maximum of 0.012 eV for the nonplanar **IV**. For that compound, the data obtained on the gas-phase geometry are much closer to their cLR than LR counterparts, confirming the results shown in Figure 1. For computing the emission energies, ω_{fluo}, LR geometries are generally sufficient: they give results very close to cLR structures, the differences being less than 1%; gas phase structures often yield larger discrepancies. Once again, the exception is **IV**, for which the different deformation predicted by LR leads to a much larger solvatochromic effect and absolute fluorescence energy compared to the cLR results. To confirm that this outcome remains an exceptionally large effect, we have modeled dithieno[2,3-*b*,2′,3′-*b*]thiophene (see graphical abstract), the next longer oligomer of **IV**. For that fused trimer, LR predicts a planar structure, and the cLR ω_{fluo} obtained on the LR and cLR geometries are much more similar, 3.953 and 3.994 eV, respectively.

Table 2. Relative cLR Energies (ΔE, in eV) and cLR Fluorescence Transition Energies (ω_{fluo}, in eV) Obtained for the Structures of Figure 1 Considering Three Different Optimal Geometries[a]

		geometry				
		gas		LR		cLR
compound	state (point group)	ΔE	ω_{fluo}	ΔE	ω_{fluo}	ω_{fluo}
I	B_u (C_{2h})	+0.006	3.366	+0.001	3.327	3.344
II	B_u (C_{2h})	+0.006	2.543	+0.008	2.540	2.526
III	B_2 (C_{2v})	+0.004	3.441	+0.005	3.431	3.429
IV	B (C_2)	+0.001	3.526	+0.012	3.773	3.498
V	B_{1g} (D_{2h})	+0.001	2.044	0.000	2.046	2.045
VI	B_1 (C_{2v})	+0.003	1.654	0.000	1.702	1.697

[a]All calculations at the PCM(DCM)-M06-2X/6-31G(d) level considering equilibrium (ΔE) or non-equilibrium (ω_{fluo}) limits of the PCM model. For ΔE, the optimized cLR structure is used as reference.

In summary, we have, for the first time, optimized excited-state geometries of molecules using a solvent model going beyond the linear-response approach. It turns out that (i) the geometrical changes induced by correcting the LR solvent model are often rather limited, (ii) in most cases cLR bond lengths are bracketed by their gas phase and LR counterparts, and (iii) in specific cases, non-negligible effects (> 0.2 eV) on the emission energies can nevertheless be found when going from LR to cLR. We are currently investigating (i) cyanine derivatives for which large LR/cLR differences of transition energies were previously reported[14,15] and (ii) fluorophores allowing direct theory−experiment comparisons of solvatochromic effects.

■ ASSOCIATED CONTENT

Supporting Information

6-31G(d) data for butadiene and hydrogen cyanide and Cartesian coordinates for the different molecules investigated. This material is available free of charge via the Internet at http://pubs.acs.org/.

■ AUTHOR INFORMATION

Corresponding Authors

*E-mail: benedetta.mennucci@unipi.it.

*E-mail: Denis.Jacquemin@univ-nantes.fr.

Notes

The authors declare no competing financial interest.

■ ACKNOWLEDGMENTS

S.C. thanks the European Research Council (ERC, Marches -278845) for her Ph.D. grant. D.J. acknowledges the European Research Council (ERC) and the *Région des Pays de la Loire* for financial support in the framework of a Starting Grant (Marches -278845) and a *recrutement sur poste stratégique*, respectively. B.M. thanks the ERC for financial support in the framework of the Starting Grant (EnLight -277755). This research used resources of (1) the GENCI-CINES/IDRIS (Grants c2013085117), (2) CCIPL (*Centre de Calcul Intensif des Pays de Loire*), and (3) a local Troy cluster.

■ REFERENCES

(1) Runge, E.; Gross, E. K. U. *Phys. Rev. Lett.* **1984**, *52*, 997−1000.

(2) Casida, M. E. In *Time-Dependent Density-Functional Response Theory for Molecules*; Chong, D. P., Ed.; World Scientific: Singapore, 1995; Recent Advances in Density Functional Methods Vol. *1*, pp 155−192.

(3) Laurent, A. D.; Adamo, C.; Jacquemin, D. *Phys. Chem. Chem. Phys.* **2014**, DOI: 10.1039/C3CP55336A.

(4) van Caillie, C.; Amos, R. D. *Chem. Phys. Lett.* **1999**, *308*, 249−255.
(5) Furche, F.; Ahlrichs, R. *J. Chem. Phys.* **2002**, *117*, 7433−7447.
(6) Liu, J.; Liang, W. Z. *J. Chem. Phys.* **2011**, *135*, 184111.
(7) Cammi, R.; Mennucci, B. *J. Chem. Phys.* **1999**, *110*, 9877−9886.
(8) Cossi, M.; Barone, V. *J. Chem. Phys.* **2001**, *115*, 4708−4717.
(9) Caricato, M.; Mennucci, B.; Tomasi, J.; Ingrosso, F.; Cammi, R.; Corni, S.; Scalmani, G. *J. Chem. Phys.* **2006**, *124*, 124520.
(10) Improta, R.; Scalmani, G.; Frisch, M. J.; Barone, V. *J. Chem. Phys.* **2007**, *127*, 074504.
(11) Marenich, A. V.; Cramer, C. J.; Truhlar, D. G.; Guido, C. G.; Mennucci, B.; Scalmani, G.; Frisch, M. J. *Chem. Sci.* **2011**, *2*, 2143−2161.
(12) Scalmani, G.; Frisch, M. J.; Mennucci, B.; Tomasi, J.; Cammi, R.; Barone, V. *J. Chem. Phys.* **2006**, *124*, 094107.
(13) Chibani, S.; Le Guennic, B.; Charaf-Eddin, A.; Laurent, A. D.; Jacquemin, D. *Chem. Sci.* **2013**, *4*, 1950−1963.
(14) Chibani, S.; Charaf-Eddin, A.; Le Guennic, B.; Jacquemin, D. *J. Chem. Theory Comput.* **2013**, *9*, 3127−3135.
(15) Chibani, S.; Charaf-Eddin, A.; Mennucci, B.; Le Guennic, B.; Jacquemin, D. *J. Chem. Theory Comput.* **2014**, *10*, 805−815.
(16) Frisch, M. J.; Trucks, G. W.; Schlegel, H. B.; Scuseria, G. E.; Robb, M. A.; Cheeseman, J. R.; Scalmani, G.; Barone, V.; Mennucci, B.; Petersson, G. A.; Nakatsuji, H.; Caricato, M.; Li, X.; Hratchian, H. P.; Izmaylov, A. F.; Bloino, J.; Zheng, G.; Sonnenberg, J. L.; Hada, M.; Ehara, M.; Toyota, K.; Fukuda, R.; Hasegawa, J.; Ishida, M.; Nakajima, T.; Honda, Y.; Kitao, O.; Nakai, H.; Vreven, T.; Montgomery, J. A., Jr.; Peralta, J. E.; Ogliaro, F.; Bearpark, M.; Heyd, J. J.; Brothers, E.; Kudin, K. N.; Staroverov, V. N.; Kobayashi, R.; Normand, J.; Raghavachari, K.; Rendell, A.; Burant, J. C.; Iyengar, S. S.; Tomasi, J.; Cossi, M.; Rega, N.; Millam, J. M.; Klene, M.; Knox, J. E.; Cross, J. B.; Bakken, V.; Adamo, C.; Jaramillo, J.; Gomperts, R.; Stratmann, R. E.; Yazyev, O.; Austin, A. J.; Cammi, R.; Pomelli, C.; Ochterski, J. W.; Martin, R. L.; Morokuma, K.; Zakrzewski, V. G.; Voth, G. A.; Salvador, P.; Dannenberg, J. J.; Dapprich, S.; Daniels, A. D.; Farkas, O.; Foresman, J. B.; Ortiz, J. V.; Cioslowski, J.; Fox, D. J. *Gaussian 09*, revision D.01.; Gaussian Inc.: Wallingford, CT, 2009.
(17) Banerjee, A.; Adams, N.; Simons, J.; Shepard, R. *J. Phys. Chem.* **1985**, *89*, 52−57.
(18) We have used ethylene as a test molecule. We have first checked that the computed forces actually corresponded to numerical derivatives of the cLR energies obtained "by hand." Next, we have performed a manual scan of the double bond length with vertical cLR and confirmed that the minimal point was indeed the one reached at the end of the corresponding geometry optimization.
(19) Note that for butadiene, the first excited state is not planar, but this constraint was applied to avoid problematic convergence of the calculations.
(20) Zhao, Y.; Truhlar, D. G. *Theor. Chem. Acc.* **2008**, *120*, 215−241.
(21) Li, R.; Zheng, J.; Truhlar, D. G. *Phys. Chem. Chem. Phys.* **2010**, *12*, 12697−12701.
(22) Jacquemin, D.; Zhao, Y.; Valero, R.; Adamo, C.; Ciofini, I.; Truhlar, D. G. *J. Chem. Theory Comput.* **2012**, *8*, 1255−1259.
(23) Jacquemin, D.; Planchat, A.; Adamo, C.; Mennucci, B. *J. Chem. Theory Comput.* **2012**, *8*, 2359−2372.
(24) Isegawa, M.; Peverati, R.; Truhlar, D. G. *J. Chem. Phys.* **2012**, *137*, 244104.
(25) Leang, S. S.; Zahariev, F.; Gordon, M. S. *J. Chem. Phys.* **2012**, *136*, 104101.
(26) Charaf-Eddin, A.; Planchat, A.; Mennucci, B.; Adamo, C.; Jacquemin, D. *J. Chem. Theory Comput.* **2013**, *9*, 2749−2760.
(27) Laurent, A. D.; Jacquemin, D. *Int. J. Quantum Chem.* **2013**, *113*, 2019−2039.